FLOW-INDUCED TONES IN A DEEP PERIODIC CAVITY

Joachim Golliard
Laboratoire d'Acoustique - Le Mans Université (LAUM)
Centre de Transfert de Technologie du Mans (CTTM)
Le Mans, France

Yves Aurégan
Laboratoire d'Acoustique - Le Mans Université (LAUM)
Le Mans, France

ABSTRACT

This paper reports a set of experiments with a chamber made of a succession of 10 deep cavities. This periodic geometry creates a bandgap of forbidden frequencies for which transmission of sound is not possible. This behaviour is first investigated with some measurements and simulations of the transmission coefficients. When a low-Mach number flow is added through the chamber, small changes on the transmission coefficients are observed. Particularly, the transmission coefficient can become larger than one at some frequencies, indicating a possible whistling of the cavities when installed in favourable conditions. The frequency range of amplification depends on the flow velocity following a nearly constant Strouhal number for the lowest velocities, but when reaching the range of forbidden frequencies, the amplification stops. A second set of measurements is reported where the cavity, installed between two anechoic terminations, is submitted to a mean flow of increasing velocity. Whistling tones are observed, once again following the Strouhal number dependency until the bandgap, but a tone is also observed right in the middle of the bandgap. This unexpected behaviour is related to azimuthal modes in the cavities.

1. INTRODUCTION

Periodic structures have interesting properties regarding acoustic propagation. One of the most striking properties is the fact that propagation is not possible in certain frequency ranges. In the limiting case of infinitely long structures, this can be illustrated through the dispersion relation of propagation in the equivalent continuous medium. The dispersion plots exhibit frequency bands (called bandgaps) for which no modes with a real wavenumber exist, which means that acoustic propagation is not possible in these frequency bands.

Even in the case of a finite number of repetitions, such band gaps can be observed. A simple illustration can be given where a number of closed side-branches is considered. If only one side branch of length L is present, this creates a filter which prevents propagation at a single frequency (and its odd harmonics) corresponding to a wavelength equal to four times the length of the side branch. This can be illustrated by the transmission coefficient (ratio of transmitted to incident wave amplitude) which is zero at a single frequency (blue line in Figure 1) for this friction-less model prediction. Now consider two side branches are placed at short distance from each other, compared to the acoustic wavelength. In this case, the region of low transmission splits in two: there are now two acoustic modes corresponding to (1) an in phase oscillation of the two side branches and (2) an out of phase oscillation of the two side branches. The frequency of the first mode is very close to that of the isolated side branche resonance. The out of phase oscillation mode has a lower resonance frequency, because the fluid between the two branches provides an additional added mass to the system, compared to the single side branch. The split is thus not centred around the low-transmission frequency of a single side-branch (red line in Figure 1). This has the effect of widening the range of frequencies where transmission is not possible. When additional (identical) side branches are added in a periodic pattern, the frequency range without transmission further increases (yellow line in Figure 1, for 5 side branches spaced by half of their length). The other effect, typical of finite periodic systems, is to add a number (equal to the number of side branches minus one) of transmission minima at frequencies just under the wide minimum centerd at $L = \lambda/4$.

A similar effect is observed when considering the transmission coefficient of a main pipe traversing a periodic succession of axisymmetric cavities at their centreline. In this case, the acoustic plane waves in the main pipe couple with the radial modes of the cavities which have a pressure minimum at their centre,

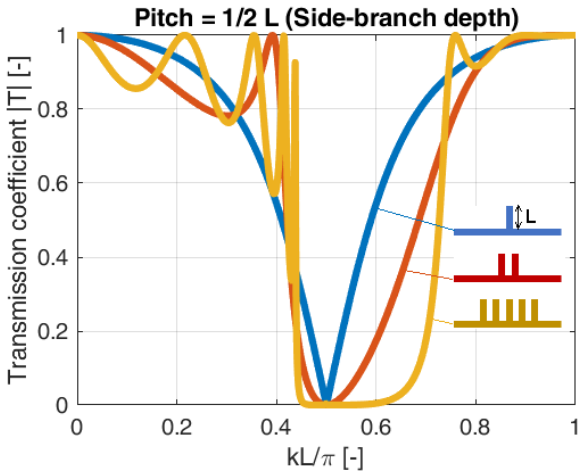

Figure 1. Transmission coefficient due to 1 (blue line), 2 (red line) or 5 (yellow line) side branches in a main pipe. The side branches have the same diameter as the main pipe and are separated by half of their depth for this illustration.

as for the quarter-wavelength modes in side-branches which have a minimum pressure at the connection with the main pipe. On the other hand, azimuthal modes in the cavities have a zero-averaged acoustic flux across any centred disk (including the one representing the section of the main pipe) and can therefore not couple with the plane waves in the main pipe (as would be the case with the out-of-phase modes of a similar array with axially opposed side branches). This case, with 10 deep axisymmetric cavities, will be considered in this paper and the transmission coefficient will be displayed in section 3, Figure 4. It shows the same features as the transmission coefficient shown in Figure 1.

The other side of the problem considered in this paper is the flow-induced pulsations which can be observed when a resonant cavity is exposed to a grazing flow over its opening. This phenomenon is observed in multiple situations, from the low-frequency buffeting in a car with an open window or roof to the flow-induced pulsations in pipe systems (Tonon et al, 2011; Ziada et al, 2013). In most of these problems, vorticity shedding occurs at a single location where acoustic resonances present a velocity maximum, which favours the flow-sound interaction and leads to the self-sustained oscillations. The amplification of sound at this single location can be very strong as it couples efficiently with a local, trapped mode. A slightly different kind of flow-induced pulsations occur with distributed "sources" coupling with global modes. This is for example observed in corrugated pipes (Burstyn, 1922; Cermak, 1924; Belfroid et al, 2007), where the amplification of sound is weaker but distributed along a large part of the system. Indeed, in this case, identical cavities are found on the full length of the pipe. The problem can then be partly considered as local, on the scale of a cell containing a single cavity, or a few cavities. Propagation of acoustic waves should take into account the attenuation due to visco-thermal losses and the amplification due to the interaction with vorticity in presence of main flow. For a very long pipe with little radiation losses, the balance between the two mechanisms is local. When the balance is exact in the linear domain, an acoustic wave can propagate infinitely without losses (Golliard et al, 2020). If the amplification is larger than the losses, the acoustic wave propagating in the corrugated pipe increases until it reaches its end where a discontinuity (typically the connection to a smooth pipe, a section change, a side branch or an open end, all creating a non-zero reflection coefficient) will reflect part of it which will propagate back in the corrugated pipe where it will be amplified again before reaching the other end of the pipe. The occurrence of flow-induced pulsations then depends on the balance between the amplification through the pipe and the radiation losses (or in other words "reflection losses"). Once the amplification is larger that the losses, the energy balance is ensured by non-linear saturation of the amplification by the vorticity (Nakiboğlu et al, 2011).

The onset of flow-induced whistling in a distributed system as the corrugated pipe is thus in essence linked to the acoustic propagation along the pipe, which can be amplified by the interaction with the flow.

The case considered in this paper shows features of both local and distributed sound-flow interaction in the resonator. With a grazing flow through the periodic cavity shown in Figure 2, vorticity develops over each of the 10 cavity openings, as in a corrugated pipe. Since the effective speed of sound in the main pipe is considerably reduced at certain frequencies due to the cavities (Aurégan et al, 2015), the periodic system becomes acoustically long and the propagation along the periodic structure should be considered. Thus, the resonator is extended (on the acoustic point of view) and the region where flow-sound interaction occurs is distributed along the extend of this resonator. On the other hand, the vorticity regions are in close proximity of each other. Therefore, the flow-induced whistling in such a periodic cavity can have properties corresponding to both systems with single-region vorticity or to distributed-vorticity systems. Indeed, depending on the thickness of the walls compared to the cavity width (and thus on the distance between the vorticity-regions), there can be significant hydrodynamic interaction between suc-

cessive cavities. The hydrodynamic instability leading to sound amplification can be a global hydrodynamic behaviour (Aurégan et al, 2008) or developing across each of the cavities, with of without interaction between successive cavities (Ziada et al, 1992; Derks et al, 2004; Nakiboğlu et al, 2011). In the last case, the synchronisation between the cavities is ensured by the acoustic feedback. Furthermore, even a single cavity can show whistling in certain cases (Mohamed et al, 2011). Furthermore, it can be expected that the band-gap of forbidden frequencies for propagation plays a role in the whistling behaviour of the system.

In the following, the flow-induced whistling in a periodic cavity will be investigated experimentally. First, the geometry is presented in more details in Section 2. The transmission through the cavity is reported in Section 3. Last, the measurements of whistling in presence of flow are presented and discussed in Section 4.

2. GEOMETRY OF THE PERIODIC CAVITY

A sketch of the periodic cavity geometry is provided in Figure 2. It is a periodic structure installed in a main pipe of 30 mm diameter. It consists of 10 successive identical axisymmetric cavities. The cavities are 7 mm wide, 55 mm deep and are separated by rigid disks of 5 mm with sharp edges. The pitch of the periodic structure is thus 12 mm.

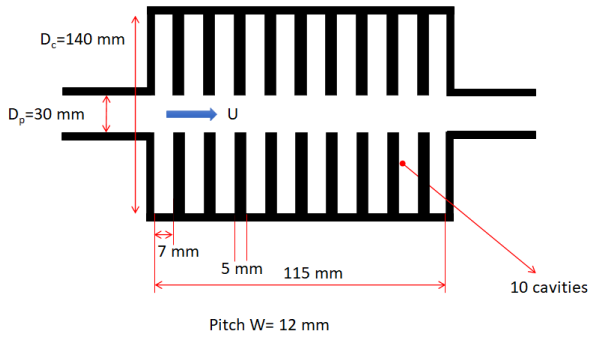

Figure 2. Sketch and dimensions of the periodic cavity.

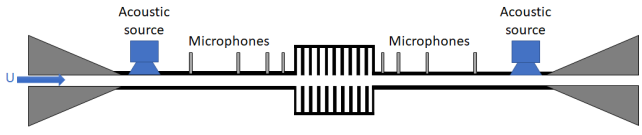

Figure 3. Sketch of the experimental setup for measurement of the scattering matrix.

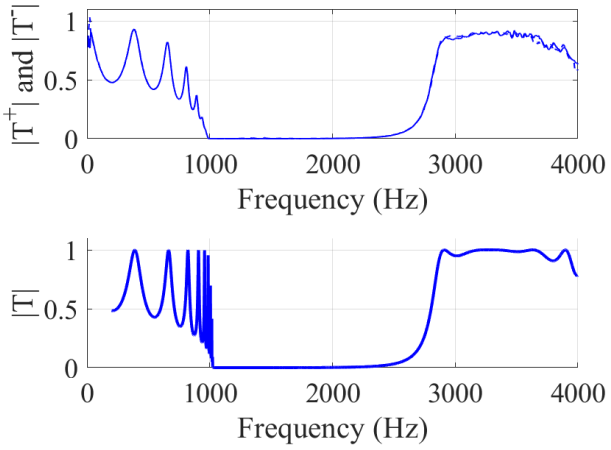

Figure 4. Measured (upper plot) and computed (lower plot) transmission coefficient due to the cavity displayed in Figure 2 without flow.

3. TRANSMISSION COEFFICIENT OF THE CAVITY

The setup for the measurement of propagation through the cavity is sketched in Figure 3. It was described in details in (Aurégan et al, 2003). It is designed to measure the scattering matrix of an element mounted in the main pipe of 30 mm inner diameter without flow or in presence of a steady flow. The central part consists of two measuring pipes equipped with each 4 microphones located upstream and downstream of the object to be characterised. Acoustic sources can be used to create an incident field coming either from the upstream side of the downstream side. Two anechoic terminations isolate this central part from the compressor located upstream and from the outlet downstream. The compressor can create a mean flow up to M = 0.35.

3.1. Transmission coefficient without flow

The measured transmission coefficient of the cavity is displayed in Figure 4. As discussed in the introduction, it shows similar features to a periodic succession of side branches. A succession of axially-opposed side branches would actually be a better "1-dimensional counterpart" of this 3-dimensional geometry, but the simplification provides a good illustration as far as the features discussed in the following are concerned. First, a frequency range is observed, between 1000 Hz and $\pm$2500 Hz, where sound waves are not transmitted by the cavity. It has to be noted that the attenuation is of the order of 70 dB over a length of only 115 mm. A second feature similar to the periodic array of side branch is the presence of

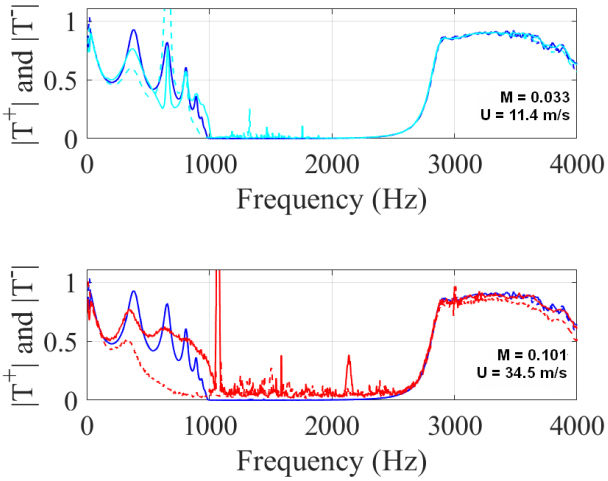

Figure 5. Transmission coefficient measured at M = 0.033 (11.4 m/s, light blue lines, upper plot) and M = 0.101 (34.5 m/s, red lines, lower plot). The results without flow are indicated for reference (dark blue lines) on all the plots. The continuous lines represent T^+ and the dashed lines represent T^-.

transmission minima around this band gap of forbidden frequencies. Five minima are very obvious on the low-frequency side, and a sixth can be suspected. On the computed transmission coefficient (lower plot of Figure 4), the number of transmission minima is nine, corresponding to the number of cavities minus one. The computation is done with the lossless acoustic solver in COMSOL. Note that, contrary to the computed transmission coefficient, the measured transmission coefficient does not pass by the value one (corresponding to perfect transmission) between theses minima. This is due to visco-thermal losses which are not taken into account in this simulation. The losses (and the resulting very small widening of the peaks and minima) are also the reason not all the minima can be observed in the measured transmission coefficient.

3.2. Transmission coefficient with flow

The transmission coefficient has also been measured with flow through the main pipe and are reported in Figure 5. One can first observe that the transmission is not reciprocal any more: The upstream and downstream transmission coefficients are not equal at low frequencies. Second, some additional damping is observed, lowering the transmission and spreading slightly the transmission lobes at low frequencies. Furthermore, the lower edge of the bandgap is shifted by the flow: towards lower frequencies for the transmission in upstream direction (T^-) and towards higher frequencies for the transmission in downstream direction (T^+). Last, for a frequency band which depends on the flow velocity, the transmission coefficient can increase and even becomes larger than one, which indicates amplification. It is noticeable that this occurs both for T^- and T^+ at the lowest velocity (but only T^- becomes greater than one) while it occurs only for T^+ for the highest velocity. This could be related to the fact that, for this velocity, the frequency range of amplification is also just on the edge of the bandgap for T^+ but very far in the bandgap for T^-.

4. WHISTLING IN PRESENCE OF FLOW

The setup for the whistling tests, sketched in Figure 6, is the same as for the measurement of the transmission coefficients, except that the acoustic sources are not used. For this set of experiments, the flow velocity has been varied from 3.3 m/s (M = 0.01) to 46.1 m/s (M = 0.14) in steps of $\pm$ 2 m/s.

The results are presented in Figure 7 as a spectrogram of pressure measured upstream and downstream of the cavity versus the Mach number. The spectrum measured upstream and downstream is also plotted for a few Mach numbers in Figure 8. One can observe in the spectrograms of Figure 7 that, for the lowest velocities, the frequency of the peak increases linearly with the flow velocity. This is typical of flow-induced noise and is characterized here by a Strouhal number $St = fW/U$ around 0.35-0.40 (with f the tone frequency, $W = 7$ mm the cavity width and U the mean-flow velocity). The frequencies at which the tones are observed in this range also correspond to the frequency range where amplification was observed in the measurements of transmission coefficients. For example, the tone occurs at 650 Hz for M = 0.033. So far, all these observations correspond to what would be observed for a "standard" corrugated pipe with shallow cavities. However, another observation can be done for this velocity range: the frequencies of the tones are discrete and correspond to the frequencies of the side lobes of possible transmission. It is also visible in the spectrum for M = 0.049 plotted in Figure 8 that smaller tones appear around the tone at 900 Hz. These smaller tones correspond to the side lobes of possible transmission in Figure 5.

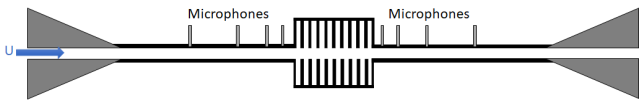

Figure 6. Sketch of the experimental setup for measurement of the whistling with flow.

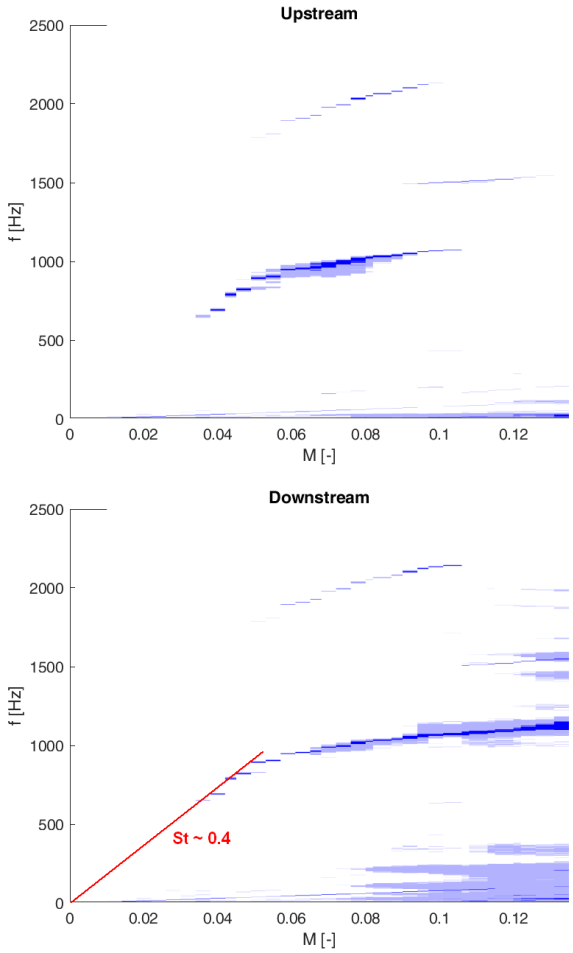

Figure 7. Spectrogram showing the flow-dependence of the noise measured upstream (above) and downstream (below) of the cavity.

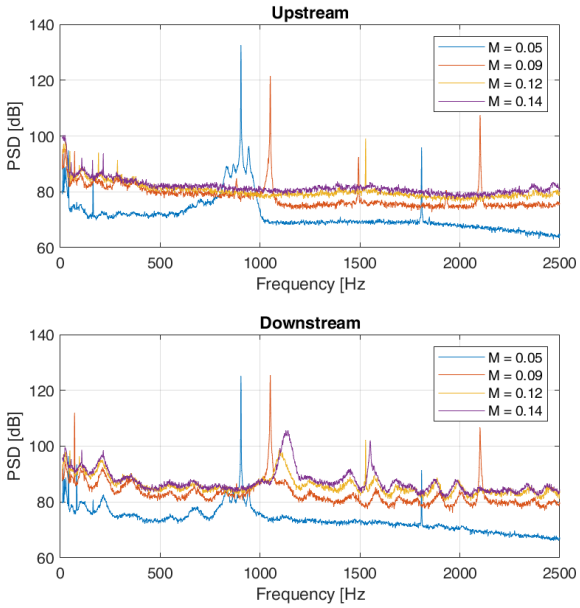

Figure 8. Spectra of the noise observed upstream (upper plot) and downstream (lower plot) of the cavity at different flow velocities.

For a (short) corrugated pipe, the discrete frequencies would be imposed by the resonant frequencies of the pipe (and thus by its total length) (Golliard et al, 2010; Nakiboğlu et al, 2010).

For velocity above M = 0.05, the Strouhal-number dependency rule does not apply any more. Indeed, the frequency of the tone only increases very slightly above 1000 Hz. For example, the tone is at 1050 Hz for M = 0.09 in Figure 8. On the downstream side, the peak widens and its amplitude decrease for higher velocities, while it disappears altogether on the upstream of the cavity. The limit of 1000 Hz corresponds to the limit of the bandgap of possible propagation and it was observed in preceding section that it increases slightly for streamwise propagation when the flow velocity increases, while it decreases for the propagation against the flow velocity (see Figure 5). This indicates that the forbidden-frequency bandgap prevents the tone from appearing. At certain flow velocities (*i.e.* M = 0.12, 0.135), the vorticity still amplifies the sound in the streamwise direction (creating the wider "bumps" around 1100 Hz – 1150 Hz measured downstream) but the wave reflected at the downstream side of the cavity then cannot propagate backwards (note that the "bumps" are not visible in any way on the upstream side).

However, some tones are also present in the frequency range of the bandgap (1000-2500 Hz). If we ignore the harmonic of the tone previously discussed, we still find a more intriguing tone observed around 1500 Hz for Mach numbers between 0.09 and 0.12 (measured by the upstream microphones) and between 0.11 and 0.15 (measured by the downstream microphones). To interpret the existence of this tone, one has to come back again to the transmission coefficient of the periodic cavity. As was discussed above, the band gap between 1000 Hz and 2500 Hz is due to the periodic structure made of deep axisymmetric cavities. In the present case, the interaction between the first radial mode of each of the cavities create the bandgap couple. Using the analogy of a periodic array of closed side branches given in the introduction, this corresponds to interaction between their quarter-wavelength resonances. A similar interaction between the modes of the individual cavities can also happen, but for the azimuthal modes. For these modes, the average acoustic flux across any centred circular section is null, which means that these modes are trapped in the cavities: They do not couple with the plane waves in the main pipe and therefore should

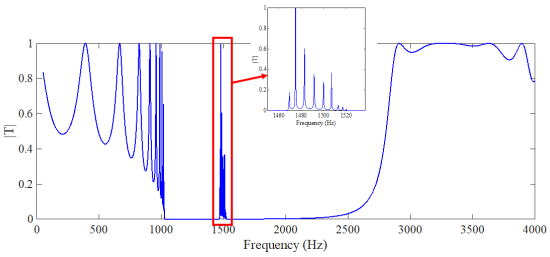

Figure 9. Transmission coefficient computed for a periodic cavity similar to the cavity displayed in Figure 2, but with the main pipe off-centre by 1 mm.

not have any influence on the transmission coefficient for plane waves. However, any small disturbance might allow some coupling. For example, the computation of the transmission coefficient was repeated with a very small modification of the geometry: the main pipe is placed 1 mm off-centre of the ten cavities. As seen in Figure 9, this creates a frequency band around 1500 Hz (or to be more precise, a succession of nine narrow frequency bands, as illustrated in the inlet of the figure) where propagation is possible. It is not expected that the cavity used for the measurements is so much off-centred, but the disturbance allowing the coupling might also come from a smaller difference, or from an asymmetry of the flow in the main pipe. At any rate, the frequency of the tone observed around 1500 Hz corresponds to this band of allowed frequencies. Flow-induced tones can be associated with trapped azimuthal modes, at least in a single shallow axisymmetric cavity, as reported by Aly et al (2010).

5. CONCLUSIONS

In this paper, flow-induced whistling observed downstream and upstream of a periodic cavity was investigated. The periodic cavity is made of a succession of 10 axisymmetric cavities spaced by a constant pitch. For low flow velocities, the frequency of the tone shows a Strouhal-number dependency characteristic of flow-induced whistling created by vorticity shedding. The phenomena are very similar to what would be observed for a corrugated pipe made of a succession of shallow cavities. However, as the flow-velocity increases, the frequency of the tone comes in a region where acoustic propagation is not possible due to periodic nature of the cavity creating a band of forbidden frequencies. This reduces and eventually eliminates the tone. Yet, a tone is observed in the bandgap of forbidden frequencies, which can be associated to the opening of an band of allowed frequencies by the presence of azimuthal modes in the cavity.

6. REFERENCES

K. Aly, S. Ziada, 2010, Flow-excited resonance of trapped modes of ducted shallow cavities, *Journal of Fluids and Structures* **26** (1) 92–120.

Y. Aurégan and M. Leroux, 2003, Failures in the discrete models for flow duct with perforations: An experimental investigation, *Journal of Sound and Vibration*, **265**(1) 109–121.

Y. Aurégan and M. Leroux, 2008, Experimental evidence of an instability over an impedance wall in a duct with flow, *Journal of Sound and Vibration*, **317** 432–439.

Y. Aurégan and V. Pagneux, 2015, Slow sound in lined flow ducts, *The Journal of the Acoustical Society of America*, **138**(2) 605–6013.

S. Belfroid, D. Shatto, and M. Peters, 2007, Flow Induced Pulsations Caused by Corrugated Tubes, *Procedings of ASME Pressure, Vessels and Piping Conference, San Antonio, TX*.

W. Burstyn, 1922, Eine Neue Pfeife (A New Pipe), *Z. Tech. Phys. (Leipzig)* **3** 179–180.

P. Cermak, 1924 Uber die Tonbildung in Luftdurch-Strömten Röhren (On the Production of Tone in an Air-Flows Through Tubes), *Physikalische Zeitschrift*, **25** 121–130.

M. M. G. Derks and A. Hirschberg, 2004, Self-sustained oscillation of the flow along Helmholtz resonators in a tandem configuration, *Proceedings of FIV2004, Paris*.

J. Golliard, D. Tonon, 2010, Whistling of Short Corrugated Pipes: Experimental Investigation of the Source Locations *Proceedings of the 16th AIAA/CEAS Aeroacoustics Conference, 2010, Stockholm, Sweden*

J. Golliard, Y. Aurégan, T. Humbert, 2020, Experimental study of plane wave propagation in a corrugated pipe: Linear regime of acoustic-flow interaction, *Journal of Sound and Vibration* **472** 115–158.

S. Mohamed, H. Graf, S. Ziada, Aeroacoustic Source of a Shallow Cavity in a Pipeline, 2011 *Proceedings of the ASME 2011 Pressure Vessels and Piping Conference Volume 4: Fluid-Structure Interaction. Baltimore, Maryland, USA*.

G. Nakiboğlu, S. Belfroid, J. Willems, A. Hirschberg, 2010, Whistling behavior of periodic systems: Corrugated pipes and multiple side branch system, *International Journal of Mechanical Sciences* **52** (11), 1458–1470.

G. Nakiboğlu, S. Belfroid, J. Golliard, A. Hirschberg, 2011, On the whistling of corrugated pipes: effect of pipe length and flow profile, *Journal of Fluid Mechanics* **672** 78–108.

G. Nakiboğlu and A. Hirschberg, 2012, Aeroacoustic power generated by multiple compact axisymmetric cavities: Effect of hydrodynamic interference on the sound production, *Physics of Fluids* **24**.

D. Tonon, A. Hirschberg, J. Golliard, S. Ziada, 2011, Aeroacoustics of Pipe Systems with Closed Branches. *International Journal of Aeroacoustics* **10**(2–3), 201–275.

S. Ziada and E. T. Bühlmann, 1992, Self-excited resonances of two side-branches in close proximity, *Journal of Fluids and Structures* **6**(5), 583–601.

S. Ziada and P. Lafon, 2014, Flow-Excited Acoustic Resonance Excitation Mechanism, Design Guidelines, and Counter Measures. *ASME. Appl. Mech. Rev.* **66**(1).